



Research Article

From purposeless residues to biocomposites: A hyphae made connection

Isabel Enriquez-Medina^a, Andres Ceballos Bermudez^{a,b}, Erika Y. Ortiz-Montoya^{a,b},
Carlos Alvarez-Vasco^{a,b,*}

^a Department of Biological Sciences, Bioprocesses and Biotechnology, Universidad ICESI, Calle 18 No, 122-135, Cali, Colombia

^b Centro Biolnc, Universidad ICESI, Cali, Colombia

ARTICLE INFO

Keywords:

Fungal mycelium
Biocomposites
Agroindustrial waste
Pleurotus ostreatus
Trametes elegans

ABSTRACT

Biocomposites create attractive alternatives to match packing needs with available agricultural residues. Growing native fungal strains developed a mycelium biocomposite over a mixture of Peach Palm Fruit Peel Flour and Sugar Cane Bagasse Wet Dust. A methodology was proposed to analyze their main characteristics: 1) morphological, 2) chemical, and 3) biodegradability. 1) SEM analysis evidenced the structural change of the dried vs pressed material and mycelium morphology for both species. 2) The ratio lignin:carbohydrate showed that *P. ostreatus* degrades the cellulose-hemicellulose fraction of the substrate at a higher rate than *T. elegans*, and 3) the curve BMP indicated that these materials are readily biodegradable with a maximum yield of 362,50 mL biogas/g VS. An innovative tangible valorization strategy based on mass balances is also presented: from just 50 kg of peel flour, up to 1840 units can be manufactured, which could pave the way for a more sustainable future.

1. Introduction

The current unsustainable production of polymers and the increasing generation of agricultural residues has been a recognized environmental issue. Biocomposites have emerged as an attractive alternative to match current packing needs with available agricultural residues to fulfill the 2030 ONU agenda for Sustainability Development Goals (SDGs) by producing greener materials [1] and promoting an industrial symbiosis by articulating secondary flows between separate industrial organizations [2,3]. This paper analyses a biotechnological strategy to transform and give value to agricultural residues from two different industries in Colombia to obtain prototypes of mycelium biocomposites growing Colombian native fungal strains.

In Colombia, agricultural activities generate around 73 million tons/year of residual biomasses [4] and only a small percentage is use, mainly as compost. However, there is a diversity of unexplored agricultural residues [5], usually due to a low nutritional value [5]. This tropical country also has a wide diversity of fungi species; around 7273 species have been identified, but the number of species is estimated to be close to 240,000, according to a 2021 report. From the identified fungi species in Colombia, 184 species have been reported as useful for food, while 110 species have been reported as helpful in traditional Colombian medicine, and only 48 species have been reported as useful in biotechnological applications [6]. Therefore, Colombia has low indicators for

reported identified fungal species but even lower numbers for their potential biotechnological use.

Concerning mycelium biocomposites, they are produced from solid-state fermentation (SSF) of white-rot fungi on agricultural residues. Fungi growth occurs through the secretion of extracellular enzymes, mainly oxidoreductases and hydrolases, that help degrade the polymers present in the cell wall of plant biomass (lignin, cellulose, and hemicellulose) [7]. Then, the fungus uses these compounds as a primary source of carbon and energy [8]. It has been described that the mechanism usually start with lignin degradation [9]. The result is a light-weight material consisting of a three-dimensional interwoven network of natural reinforcing fibers composed by the spent raw material and mycelial hyphae, which acts as a natural binder [7]. Due to their organic composition, these materials can be degraded naturally after use, allowing for a fully circular production model [8], thus providing resilient and efficient solutions to current environmental challenges [9].

Recent research has demonstrated the potential of fungal mycelium to produce biocomposites as substitutes for traditional non-renewable polymers [10], extending the applications to diverse fields such as materials, biotechnology, engineering, architecture, art, and design. In this sense, the diversification of uses includes building blocks, insulation panels, packaging, leather, and textiles [11]. Due to their low density, impact resistance, low thermal conductivity, and low cost [10], these materials are starting to impact several market niches (*i.e.*, automotive,

* Corresponding author.

E-mail address: caalvarez@icesi.edu.co (C. Alvarez-Vasco).

<https://doi.org/10.1016/j.btre.2023.e00807>

Received 27 April 2023; Received in revised form 26 June 2023; Accepted 27 June 2023

Available online 1 July 2023

2215-017X/© 2023 The Author(s). Published by Elsevier B.V. This is an open access article under the CC BY-NC-ND license (<http://creativecommons.org/licenses/by-nc-nd/4.0/>).

construction, and interior design) [11] intensifying the interest in the creation of startups and green businesses that pluralized the approaches to mycelium as a scalable and sustainable raw material. [12]. For instance, companies such as Ecovative, Mycoworks, and MOGU are exponents of biocomposites whose niches are growing to new applications.

Several studies have indicated that biocomposites characteristics (e. g., those that are used to determine their final application depend directly on mainly five variables: 1) Fungal species (that produce the mycelium), 2) Substrates, 3) the interaction between mycelium and substrates, 4) Manufacturing processes (i.e., sterilization, drying) and 5) Post-processing (i.e., thermoprocessing) [13,14]. This paper presents a new biotechnological composite by analyzing those five variables using 1) two Colombian native fungal strains, *Pleurotus ostreatus* and *Trametes elegans*, over a mixture of 2) Peach Palm Fruit Peel Flour (main substrate), and a recalcitrant residue of Sugar Cane Bagasse Wet Dust from paper industry (support substrate), 3) the interaction between native fungal species and substrates 4) after sterilization, SSF, and drying, and 5) with or without thermoprocessing. As far as we know, this residue mixture has not been used before on obtaining mycelium biocomposites. Although, the growth of fungal biomass on agricultural residues to obtain materials has been studied, their application is largely unexplored [3], and so far, local residues as well as Colombian native strains, have not been researched for related biotechnology applications.

Although biocomposites are very attractive, they still represent a challenge given their heterogeneous, anisotropic, and hygroscopic nature [13]. In fact, as an emerging field, the reproducibility of methodologies, and consistency of variables to analyze is not well defined. [15]. The information does not include standardized results, and they are highly variable. In this sense, biocomposites characterization has been useful in recognizing patterns between analytical methods to identify properties and perhaps applications. Used methods include: 1) Scanning Electron Microscopy (SEM) to recognize the morphology of the actors involved and their interactions, 2) Fourier Transform Infrared Spectroscopy (FTIR) to facilitate the identification of main polymers in the material (carbohydrates, lipids, proteins) and to allow a semi-quantitative monitoring of the fermentation, 3) Physical and mechanical tests such as density and flexural to visualize the landscape of applications, and 4) biodegradation analysis to evaluate biocomposites mass loss during time and thus their potential impact in the environment.

Immersed in a country of vast biodiversity and agricultural richness, we developed a new biocomposite from two model agricultural residues and two Colombian native fungal strains. In this study, two processing alternatives after SSF are also illustrated, with drying and thermopressing operations steps, as well as morphological, chemical, and biodegradability analysis of the new biocomposite. The results provide a vision of the versatility and potential applications of biocomposites to replace traditional polymeric materials. In fact, Mycelium hyphae make possible the connection between agricultural residues and useful biocomposites. The "connective" strength of the mycelium in the transformation of new substrates not only provides an understanding of unique characteristics concerning the use of the five main variables but also "connects" a vision of agroindustries as future biorefineries of their own by-products towards a fully circular production model.

2. Experimental section

2.1. Strain and seed culture conditions

Pleurotus ostreatus (EBB-114), and *Trametes elegans* (ET-06) strains used belong to the collection of the Biochemical Engineering Laboratory of Universidad Icesi and Universidad de Antioquia. In this work, the endophytic basidiomycete *Trametes elegans* (ET-06) was isolated from the stem of *Otoba gracilipes*, in a tropical montane rainforest in Antioquia, Colombia, with GenBank Accession Numbers MT941002 [16],

while the white-rot *Pleurotus ostreatus* was isolated from a trunk of *Heliocarpus popayanensis* in Puracé, Cauca.

The stock cultures of both strains were maintained on potato dextrose agar (PDA) before use. The seed medium was prepared using wheat grains (*Triticum*), type II water, and glucose as a supplement. Wheat was soaked for 24 h for hydration and then crushed in a knife mill. Subsequently, to each petri dish was added 6 g of wheat, and 2 mL of a 5 g/L glucose solution. Petri dishes were autoclaved at 121 °C for 15 min and then allowed to cool down. The substrate was inoculated using the fungal species under a Class 2 (laminar flow) biological safety cabinet. Petri dishes were incubated at 28 ± 2 °C for up to 5 days to promote the complete colonization of grains.

2.2. Substrates conditioning for fermentation

Two agroindustrial residues from Valle del Cauca were used: 1) Sugar Cane Bagasse Wet Dust (SCB Wet Dust) was kindly provided by PROPAL S.A a paper making industry located in Yumbo, Valle del Cauca, Colombia, and 2) Peach Palm Fruit Peel Flour (PPF Peel Flour) obtained from Frudelpa S.A, a company specialized in the production and distribution of fruits from Colombian Pacific.

First, both residues were dried separately in a convection oven (BINDER FD 115) using a temperature profile from room temperature to 80 °C for 8 h until they reached a humidity of about 10%. After drying, SCB Wet Dust was sieved to obtain particle sizes between 30 and 50 mm, while PPF Peel Flour were ground using a continuous knife mill CM-20,000 (MRC Lab, UK) and passed through a 2 mm sieve to obtain the flour.

To prepare 100 g of substrates for SSF, a mixture was made using 50 g of PPF Peel flour and SCB Wet Dust. This mixture was supplemented with 2% wt CaCO₃ and DI water to reach a desired humidity of 80%. Subsequently, the mixture was added on aluminum moulds (31 cm x11cm x3,5 cm, L-W-D) and autoclaved for 15 min at 121 °C. Aluminum moulds were used for incubation.

2.3. Solid state fermentation and biocomposites post-treatment

Treatments were inoculated at 15% wt (inoculum to the substrate, on dry basis) [17]. Two inoculation techniques were used: 1) direct (wheat seed is added to the substrate) and 2) suspension with Tween 80 at 1% for *Pleurotus ostreatus* and *Trametes elegans*, respectively. The molds were covered with cellophane foil, and they were placed in an incubation chamber for ten days in darkness, at temperature of 28 +/- 2 °C and relative humidity between 80 and 85%. A second growth stage was performed. For this, all the samples were removed from the mold and they were inverted in position. These were left to grow for ten more days in the initial conditions already described to favor the transfer of gasses and, thus, the growth of the fungus on the uncolonized surface.

Once the growth period was over, thermal deactivation was performed to prevent the spread of the microorganism and possible contamination. The process consisted of drying the biocomposites in a convection oven (BINDER FD) at 105 °C for 5 h. The dry mycelium-based composites were hot pressed at ~150 °C and 125 psi for 2 min in a compression molding machine.

2.4. Substrates and biocomposites characterization

The morphology of the obtained biocomposites was examined using a ZEISS EVO 15 scanning electron microscope. Prior to the examination, a thin layer of gold/platinum was sprayed onto the samples using an SC7620 Mini Sputter Coater ion spray coater. Hyphae diameter was measured with ImageJ Software [18] and completed to analysis with OriginPro 2017 Statistical Analysis Software [19]. Additionally, scanning infrared spectroscopy (FTIR-ATR) was performed in the IR spectrophotometer Nicolet 6700, ThermoScientific using Thermo Scientific™ OMNIC™ Series software.

For the physicochemical analysis of the samples, the methodology described by Sahito et al. [20] was used by which the total solids (%TS) and volatile solids (%VS) were determined for each sample. Density was determined according to ASTM C-303 [21]. The biodegradation analysis was carried out through the anaerobic digestion of the samples in batch-type reactors of 1 L incubated at 35 °C, with continuous stirring. Each reactor was connected to a biogas fluid meter, controlled by an Arduino for biogas measurements, which, in turn, is connected to a Telar® bag for biogas collection. The process was carried out in duplicate, with the objective of determining the quantity of biogas and biomethane produced per gram of substrate (BMP). The experiment was stopped 25 days later when no change in the gasses produced was evident.

2.5. Statistical analysis

Statistical analysis was made with the Minitab 19 software package and Microsoft Excel for the biodegradability test. The normality of the data was determined following the Shapiro-Wilk test. A one-way analysis of variance (ANOVA) was used for the biodegradability test, and significant differences were considered at $p \leq 0.05$. The multiple-comparison test was determined from the Tukey test.

3. Results and discussion

3.1. Morphological characterization of biocomposites

Obtained biocomposites (Fig. 1) show different visual characteristics. For instance, *T. elegans* mycelium is translucent analogous to a thin cotton film while the mycelium of *P. ostreatus* is white, dense, and frothy. The aerial hyphae of both strains are visible on the surface of composites mainly due to higher air contact. In the composites core, where penetrating hyphae are prevalent, colonization zones growth was better in *P. ostreatus* than in *T. elegans*.

The biocomposites that followed drying post-treatment shown rough and irregular surfaces and tend to fracture in uncolonized regions. In addition, the mycelium-based composites were porous, soft and foamy to the touch. In contrast, pressed composites exhibit smooth and uniform

surfaces. They were rigid, compact and resistant to manual deformation similar to fiberboard [22]. Heat treatment allowed visualizing the effect of temperature on the appearance and morphology of the biocomposite. Fig. 1 shows the chromatic variation from white to brown of the biocomposites due to Maillard reactions involving sugars and proteins present in the cell walls of fungi and plants [23] that react due to a temperature rising. Likewise, the heat produced dehydration of the hyphae by evaporation of the water present in the cell wall and allowed the hyphae to join [24]. Thus, a compact and homogeneous mycelial network was obtained. This suggests that the post-treatment was able to modify the microporous structure of resulting composites.

SEM images of *P. ostreatus* and *T. elegans* obtained composites showed similar growth patterns. It is observed that the penetrating hyphae growth around the SCB Wet Dust (continuous and elongated structure) forming anastomoses [25], they branch randomly in all directions weaving a tridimensional mycelial network that agglomerates the natural fiber (Fig. 2).

Two characteristic types of mycelial structures are observed between the two species: *P. ostreatus* has tubular and branched hyphae in the form of thin filaments in form beta sheet with a diameter of 2,5 μm (Fig 1a and 1c) like that reported by other researchers [26]. In contrast, *T. elegans* exhibits elongated, semicontinuous hyphae with a greater amplitude in diameter (Fig 1c and 1f).

3.2. Chemical characterization of the biocomposites obtained

The chemical composition of PPF Peel Flour and SCB Wet Dust has been elucidated by different authors [27,28]. Thus, Fourier transform infrared spectrometry (FTIR) is used to analyze the lignocellulosic profiles of the substrates and its relationship with mycelial biomass growth. As seen in Fig. 3, the spectrum of the 1:1 mixture is very similar to the spectrum of SCB Wet Dust and it appears to be the predominant chemical profile. The spectrum of PPF Peel Flour reveals distinct bands associated with cellulose, lipids, proteins and pectin corresponding to numbers 1, 2-3, 4 and 5' respectively (Table 1). In particular, the intensity of band 3 is well defined for this spectrum, suggesting a lipid fraction available in this substrate. On the other hand, it is observed that peak 5' of the flour spectrum is slightly shifted to the right relative to

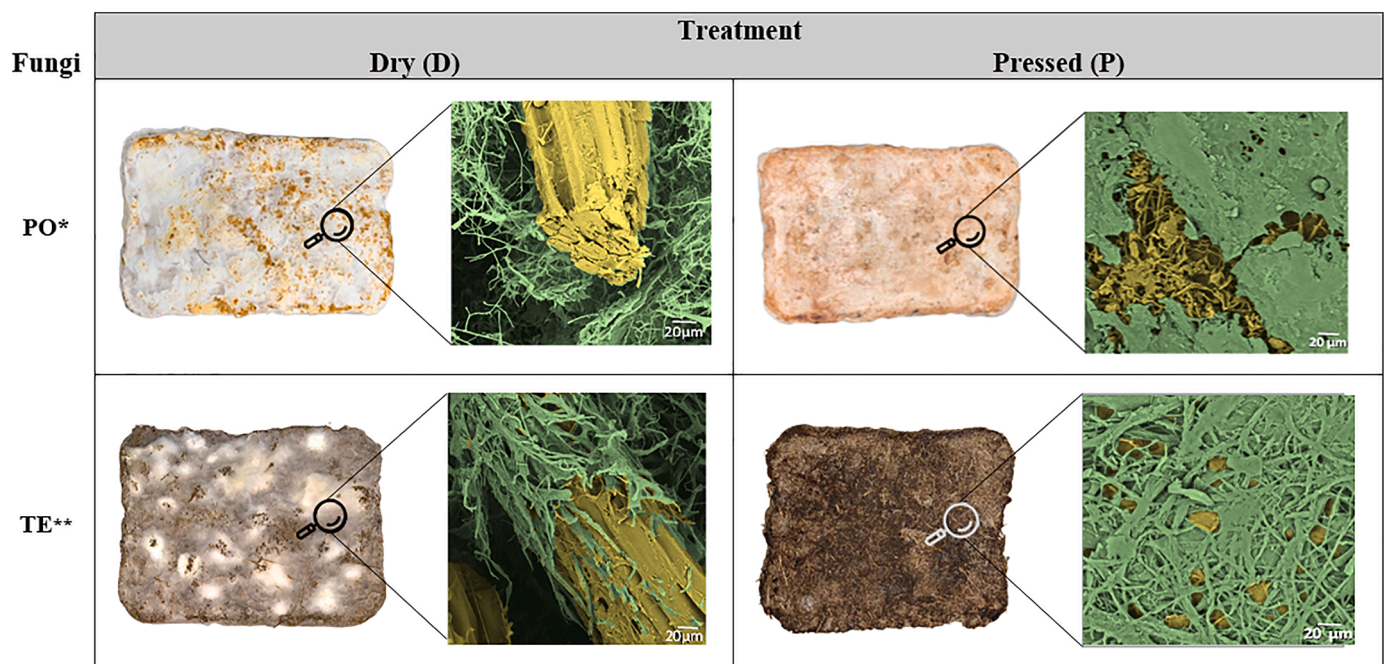


Fig. 1. Obtained biocomposites corresponded to Dry *Pleurotus ostreatus* (DPO), Pressed *Pleurotus ostreatus* (PPO), Dry *Trametes elegans* (DTE) and Pressed *Trametes elegans* (PTE). * *Pleurotus ostreatus* (PO); ** *Trametes Elegans* (TE); Images colored to highlight ■ Mycelium, ■ SCB Wet Dust.

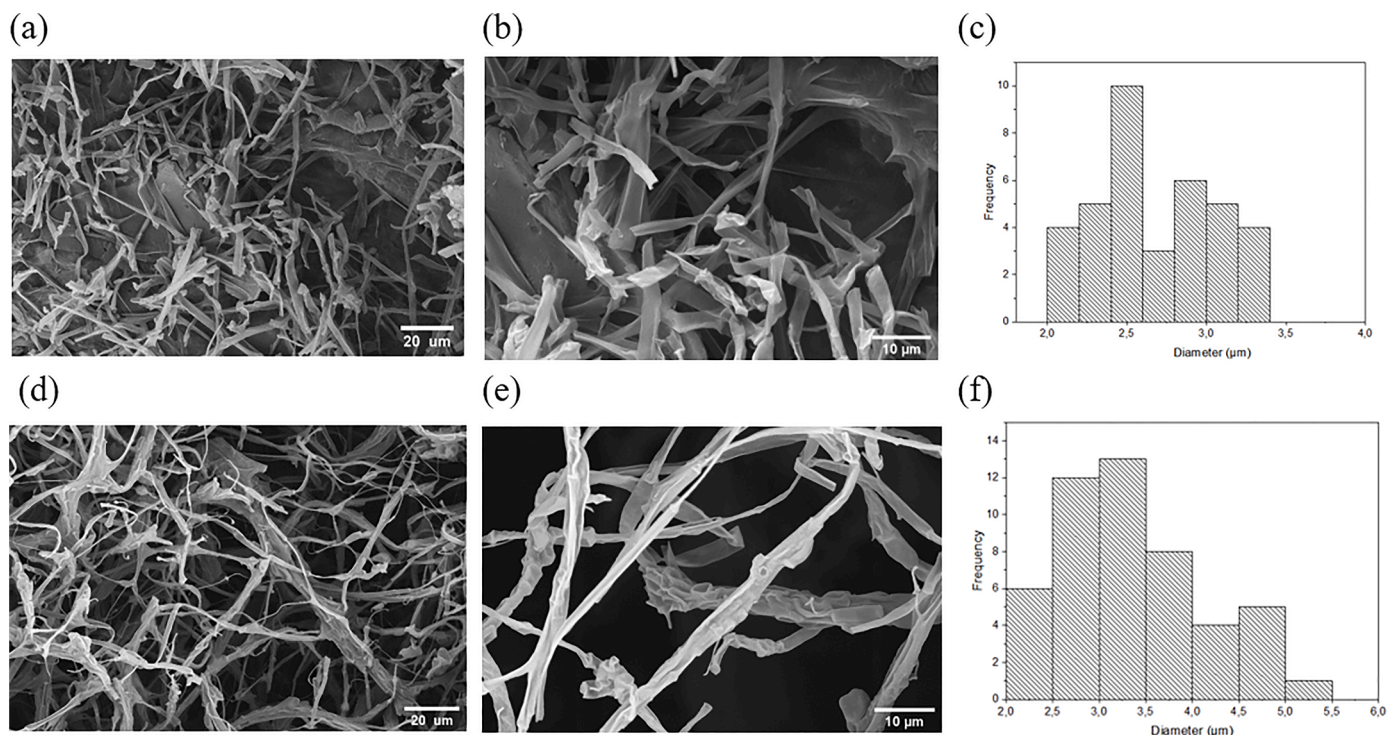


Fig. 2. SEM images of biocomposites (a) *P. ostreatus* (scale bar is 20 μm). (b) *P. ostreatus* (scale bar is 10 μm). (c) *P. ostreatus* hyphae diameter distribution with mean $2,5 \pm 0,36 \mu\text{m}$. (d) *T. elegans* (scale bar is 20 μm). (e) *T. elegans* (scale bar is 10 μm). (f) *T. elegans* hyphae filament diameter distribution with mean $3,10 \pm 0,09 \mu\text{m}$.

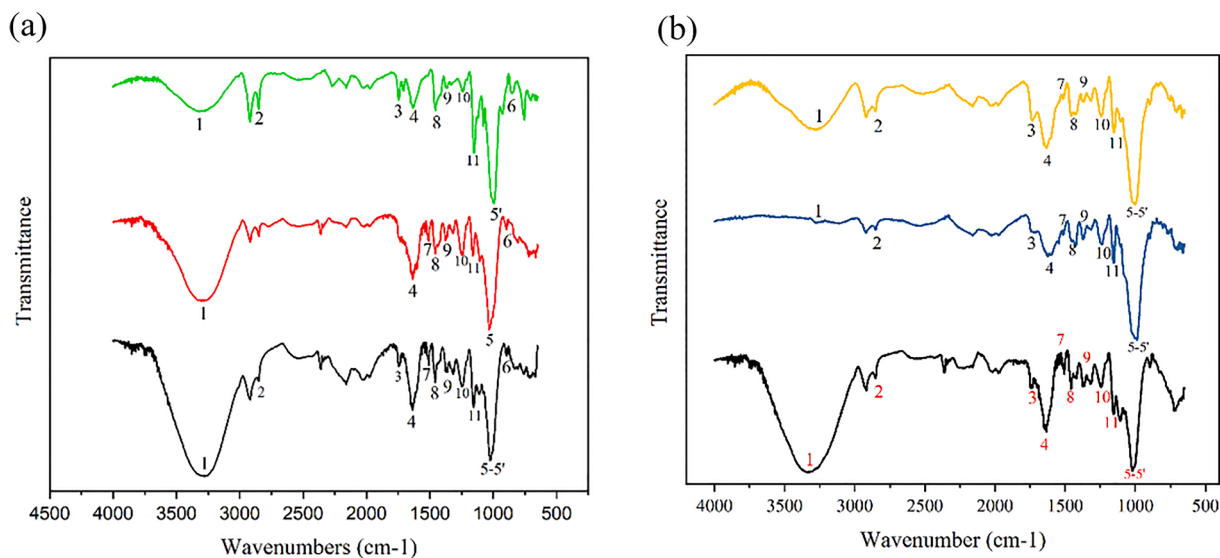


Fig. 3. FTIR-ATR spectra of biocomposites obtained. a) Substrates before being inoculated: Main assignments of PPF Peel Flour (green), SCB Wet Dust (red), Mix of PPF Peel Flour and SCB Wet Dust (black). b) Mycelium samples after growth: Main assignments of *P. ostreatus* (yellow) and *T. elegans* (blue) are included.

peak 5 present in the mixture spectrum. This is explained by the composition of Peach Palm Fruit rich in fiber (pectin and starch) which generates an intensity maximum around 1015cm^{-1} .

The spectrum of SCB Wet Dust has unique bands within the $1700\text{--}1100 \text{cm}^{-1}$ region that are associated with the presence of polysaccharides such as cellulose, hemicellulose and lignin. These are listed in Table 1 with numbers 6, 7, 8, 9, 10 and 11. A pronounced peak is observed at 4, which could be related to absorbed water given the hygroscopic nature of bagasse. Both substrates are lignocellulosic biomasses, however, PPF peel flour have distinctive and pronounced peaks (6, 9 and 11, Table 1) that are associated with more abundant and less

recalcitrant cellulose and starch. Therefore, PPF flour represents the main source of energy and carbon for cellular growth, in contrast, with the high recalcitrant value of bagasse that can be observed on bands that are related to lignin (peaks 7 and 10, Table 1).

In addition, the FTIR spectroscopy was used to observe the variation of structural carbohydrates during the mycelium growth by analyzing their functional groups. Fig. 3 shows two distinctive regions within the three spectra. The first region is located between 4500 and 1700cm^{-1} and the variation between the intensity profiles is easily identified. The mixture reaches a pronounced band at 1 suggesting a presence of cellulose in this compound. The second range well known as fingerprint

Table 1Peak assignments of the FTIR spectral bands of Peach Palm Fruit Peel Flour, Bagasse Wet Dust, *P. ostreatus*, and *T. elegans*.

Peak number	Wavenumber (cm ⁻¹)	Substrate <i>P. ostreatus</i> / <i>T. elegans</i>	PPF Peel Flour	SCB Wet Dust.	Band assignments	References
1	~3299	NA	Cellulose I	Cellulose I	O-H stretching intramolecular hydrogen bonds	[29]
2	~2854	NA	Lipids	NA	Symmetric stretching vibrations of skeletal CH and CH ₂	[30]
3	~1740	NA	Lipids	NA	Carbonyl bond vibration (—C = O)	[30]
4	~1640	NA	NA	Lignin	C = O stretching vibration in conjugated carbonyl	[31]
		NA	Protein	NA	Stretching vibration of N-linked C = O	[32]
		Chitin	NA	NA		[33]
		NA	Water	Water	H-O-H bending vibration absorbed water	[34]
5	~1036	NA	NA	Cellulose/ Hemicellulose	C—O stretching vibration	[35]
5'	~1010	NA	Pectin	NA	C-O stretching, C—C stretching pectin (C2-C3,C2-O2, C1-O1) backbone vibrations	[34]
6	895–890	NA	Cellulose	Cellulose	C—O—C stretching in β-(1 →4) glycosidic bonds	[36]
7	~1510	NA	Lignin	Lignin	C = C stretching vibration aromatic ring	[35]
8	~1458		Lignin	Lignin	CH ₂ deformation stretching	[31]
9	~1375	Chitin	NA	NA	Bending vibration of the C—H bond	[14]
			Cellulose/ Hemicellulose	Cellulose/ Hemicellulose	C-H vibrations and CH ₂ bending	[34]
10	~1245		Lignin	Lignin	C—O stretching vibration aryl group	[37]
11	~1158		Cellulose/ Hemicellulose	Cellulose/ Hemicellulose	C-O-C stretching	[37]

region located between 1500 and 400 cm⁻¹ features similar positions for most bands. However, the relative intensities of the bands vary considerably. The relative intensities of the bands are in 9 and 11 more attenuated in the *P.ostreatus* and *T.elegans* biocomposites compared to the pure mixture. This demonstrates the degradation of structural carbohydrates present in the substrate by the enzymatic mechanism of the fungus. In contrast, peaks 4 and 9 present in the two spectra of the mycelium-based composites, allow us to elucidate the appearance of a polysaccharide present in the fungal cell wall: chitin.

The relation between lignin and carbohydrates can be calculated by the association of some FTIR spectral bands [38] as shown in Fig. 4. The decrease in the lignin:cellulose ratio (I_{1510}/I_{895}) ranged from 1,47–1,41 for biocomposites obtained from *P. ostreatus* and *T. elegans*, respectively. The decrease in the lignin:cellulose ratio of both strains is lower for the band 9 compared to other carbohydrate bands 6 (Fig. 3). This indicating that both strains preferentially decayed the cellulose fraction over the hemicellulose fraction [39]. In turn, the relation of the intensities between lignin:chitin (I_{1510}/I_{1375}) is higher in *P.ostreatus* (1,17) compared to *T.elegans* (1,12) and indicates that the fungal cell wall structural compound is present in higher proportion in the composites obtained from *P. ostreatus*. This result coincides with those obtained in SEM where the mycelium of *P.ostreatus* colonizes the entire matrix of the substrate both in its core and its surface walls.

3.3. Anaerobic biodegradability analysis

After a culture period of 25 days, the biocomposites obtained from *Pleurotus ostreatus* and *Trametes elegans* were dried and characterized in terms of volatile solids, percentage of humidity and density (Table 2). The higher content of organic matter (VS) was associated with specimens obtained from *P.ostreatus* which in turn exhibited higher colonization.

Anaerobic biodegradability was defined following two methods: in terms of BMP and percentage degradation (% DEG) established according to ASTM D5526 [40], as illustrated in Fig. 5. The data for *Trametes elegans* was not reproducible and with high deviations, thus they are not included in the analysis.

Following the classification established by Remigi and Buckley [41], the biogas yield curves are close to type 1 curves and indicate that the test material is readily biodegradable. Biogas is produced with a high

Table 2

Characterization of samples for biodegradation tests.

Sample	Weight (g)	Volatile solids (%w/w)	Moisture (%)	Density (g/cm ³)
DPO	4,4	88,78%	7,24%	0,165
PPO	4,4	89,78%	6,78%	0,326

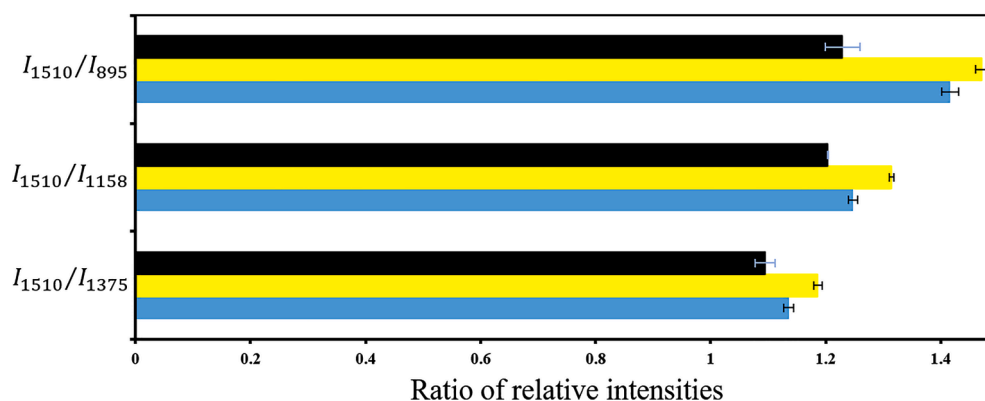


Fig. 4. Ratio of relative intensities I_{1510}/I_{895} Lignin:cellulose I_{1510}/I_{1158} Lignin:hemicellulose I_{1510}/I_{1375} Lignin:chitin Standard deviation is performed with duplicate samples (mean ± one standard deviation). ■ Mix ■ *P. ostreatus* ■ *T. elegans*.

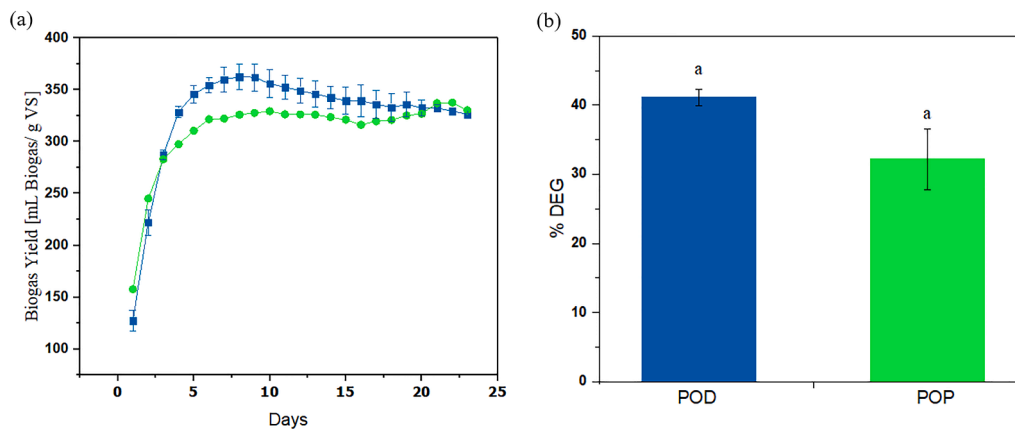


Fig. 5. Anaerobic biodegradability of *P. ostreatus* samples. (a) BMP, (b) % DEG. Standard deviation is performed with duplicate samples (mean \pm one standard deviation). Equal letters indicate no significant difference according to Tukey's test at $p \leq 0.05$. ■ *Pleurotus ostreatus* drying ■ *Pleurotus ostreatus* pressed.

slope within the first 10 days without lag phase or inhibition. The highest biogas production (362,50 and 326,09 mL biogas/g VS) was obtained during the first 8 days for dry and pressed biocomposites respectively. These results are below the theoretical yield (414.8 mL/g VS) for these lignocellulosic sources [42]. However, they range within those reported for plant materials [43,44] and suggest that these new end-of-life fungal compounds may be promising bioenergy candidates for anaerobic biorefineries.

The percentage of degradation (% DEG) of each post-treatment sample was determined by evaluating the percentage of carbon in the total substrates versus the gasses resulting from anaerobic digestion (CH₄ and CO₂). Thus, it is to be expected that biocomposites with the highest biogas yield (our case was dry *P. ostreatus*) will have the highest %DEG. Fig. 5a shows this trend. However, no significant differences were found in the data (Fig. 5b). Considering that the post-treatment included two operations, the results suggest that pressing decreases the surface area available for enzymatic attack [45] because the density doubles modifying the microporous structure of the material, as evidenced in the SEM analysis.

3.4. Relationship between raw material and biocomposites

According to the inherent characteristics of mycelium: hydrophobicity, flexibility, dimensional stability, and biodegradability [46,47] it was considered a potential application as a food packaging material, particularly for single-use cups. Fig. 6 schematizes the connection between a value-added product created with mycelium from non-purpose wastes from Valle del Cauca. Specifically, the dry mass balance is presented for Frudelpa S.A. (a local company), whose production of peels ranges around 100 kg/week. For biocomposites with a weight of 80 g as illustrated in stream 11, it is possible to manufacture approximately 1840 units from 50 kg of PPF Peel Flour. The resulting cup hydrophobicity was not analyzed in this study. However, the ratio of cup units

produced/waste utilized gives an idea of the versatility of composites that can be obtained from these renewable organic raw materials.

Our results show that Wet Dust natural fiber works mainly as support (islands) that are connected by mycelium (bridges) growing using the PPF Peel Flour as nutrients for vegetative body growth. FTIR results coupled with anaerobic biodegradability analysis showed an improvement on biodegradability of the highly recalcitrant SCB Wet Dust due to the hydrolytic action of secreted lignocellulosic enzymes by fungi strains during colonization. In addition, degradation percentage based on consumed carbon was 42.52% for *P. Ostreatus* dry and decreased to 25.43% after pressing. Pressing definitively have a negative impact on mycelium-based material biodegradation, while fungi colonization increased biodegradability. Therefore, our mycelium-based biocomposites are promissory compounds for packing. It is possible to manufacture approximately 1840 units from 50 kg of PPF Peel Flour.

4. Conclusions

Mycelium-based composites were obtained using two different species of Colombian native fungus and a novel mixture of substrate that was composed of two local agricultural residues 1) Peach Palm Fruit (PPF) Peel Flour and 2) Sugar Cane Bagasse (SCB) wet Dust. PPF Peel Flour worked mainly as carbon and energy source, while SCB Wet Dust was a support to allow mycelium growth throughout.

It was found that *T. elegans* mycelium was translucent without colored stains from the mycelium growth, therefore, maintaining the overall ivory natural color of SCB Wet Dust, regarding texture, these fungi growth developing heterogeneous hyphae structures showing some level of roughness and bumps over the surface.

P. ostreatus developed long range, thin, ramified, and discontinuous hyphae that were able to fill almost all empty spaces on the supporting substrate; its mycelium was whitish-gray and prevailed over the natural ivory color of SCB Wet Dust.

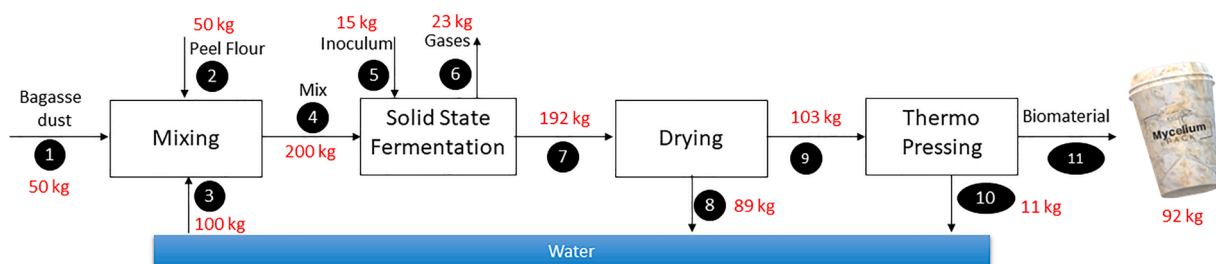


Fig. 6. Schematic diagram of the process from substrates to biocomposites detailing the dry mass balance.

Regarding native species' performance to generate the biocomposites, the IR spectra, and SEM results showed that *P. ostreatus* was the best strain because their hyphae penetrated and colonized all the supporting substrates. In addition, IR spectra show distinctive bands for quitine, cellulose, and hemicellulose, indicating that this strain consumed more substrate and produced more fungi biomass compared with the Colombian *T. elegans* strain.

Anaerobic biodegradability demonstrates that biocomposites may degrade to their simplest form (CO₂) in a range of 42.52% and 32.75% for dry and pressed materials, respectively, over a period of 25 days. As a result, pressing reduces porosity, increases density, and restricts access to substrate areas for enzymatic attack. Furthermore, the BMP indicates that these compounds are readily biodegradable under anaerobic conditions and can be used to generate bioenergy from their anaerobic digestions once they reach their final use while obtaining a less recalcitrant biomass that can be used on other applications (e.g., soil). As a result, based on the 2030 SDGs, these biocomposites have a greater potential to address existing circular economy demands in Colombia and other OCDE countries.

Mass balances and experimental results allow for estimating the rate of biocomposite production per gram of waste recovery. Thus, on a week of operation of the local industry that generates 50 kg of Peach Palm Peel as residue (*i.e.*, Frudelpa S.A), it is possible to obtain up to 1840 units of 80 gs cups made from mycelium-based composites through an additional downstream process that includes drying and thermopressing. In fact, biocomposites are very promising to transform the current unsustainable production of petroleum-based packing materials. This new alternative positions biodiversity as a source of creation and innovation for generating new products and expands the panorama of lignocellulosic biomass valorization.

Declaration of Competing Interest

The authors whose names are listed immediately below certify that they have NO affiliations with or involvement in any organization or entity with any financial interest (such as honoraria; educational grants; participation in speakers' bureaus; membership, employment, consultancies, stock ownership, or other equity interest; and expert testimony or patent -licensing arrangements), or non-financial interest (such as personal or professional relationships, affiliations, knowledge or beliefs) in the subject matter or materials discussed in this manuscript.

Data availability

Data will be made available on request.

Acknowledgements

This work was supported by Universidad ICESI through the internal financing program of the Engineering Faculty with grant number COL0039769-1102. "Conversion of residues to materials used on biodegradable packing" supported in addition by the Biochemical Engineering Department.

References

- [1] O.A. Alabi, K.I. Ologbonjaye, O.E. Alalade, O. Awosolu, Public and environmental health effects of plastic wastes disposal: a review, *J. Toxicol. Risk Assessment* 5 (2019), <https://doi.org/10.23937/2572-4061.1510021>.
- [2] L. Shi, Industrial symbiosis: context and relevance to the sustainable development goals (SDGs), (2020) 381–391. https://doi.org/10.1007/978-3-319-95726-5_19.
- [3] E. Elsacker, S. Vandeloock, A. van Wylick, J. Ruytinx, L. de Laet, E. Peeters, A comprehensive framework for the production of mycelium-based lignocellulosic composites, *Sci. Total Environ.* 725 (2020), 138431, <https://doi.org/10.1016/j.scitotenv.2020.138431>.
- [4] P.D. Cuadrado-Osorio, J.M. Ramirez-Mejía, L.F. Mejía-Avellaneda, L. Mesa, E. J. Bautista, Agro-industrial residues for microbial bioproducts: a key booster for bioeconomy, *Bioresour Technol Rep* 20 (2022), <https://doi.org/10.1016/j.biteb.2022.101232>.
- [5] CONSEJO NACIONAL DE POLÍTICA ECONÓMICA Y SOCIAL, Green growth policy. CONPES DOCUMENT 3934 OF 2018.
- [6] E. Gaya, A. Vasco-Palacios, J. Carretaro, B. Allkin, T. Cossu, L. Davis, J. D'Souza, A. Dufat, D. Hammond, M. del P-Mira, J. Morley, T. Ulian, K. White, M. Diazgranados, J. Ruff, ColFungi : colombian resources for fungi made accessible, 2021. www.newtonfund.ac.uk.
- [7] M. Haneef, L. Ceseracci, C. Canale, I.S. Bayer, J.A. Heredia-Guerrero, A. Athanassiou, Advanced materials from fungal mycelium: fabrication and tuning of physical properties, *Sci. Rep.* 7 (2017) 1–11, <https://doi.org/10.1038/srep41292>.
- [8] V. Meyer, M.R. Andersen, A.A. Brakhage, G.H. Braus, M.X. Caddick, T.C. Cairns, R. P. de Vries, T. Haarmann, K. Hansen, C. Hertz-fowler, S. Krappmann, U. H. Mortensen, M.A. Peñalva, A.F.J. Ram, R.M. Head, Current challenges of research on filamentous fungi in relation to human welfare and a sustainable bio-economy: a white paper, *Fungal Biol. Biotechnol.* 3 (2016) 1–17, <https://doi.org/10.1186/s40694-016-0024-8>.
- [9] F.S. Chambergo, E.Y. Valencia, Fungal biodiversity to biotechnology, (2016). <https://doi.org/10.1007/s00253-016-7305-2>.
- [10] M. Jones, A. Mautner, S. Luenco, A. Bismarck, S. John, Engineered mycelium composite construction materials from fungal biorefineries: a critical review, *Mater. Des.* 187 (2020), <https://doi.org/10.1016/j.matdes.2019.108397>.
- [11] M. Sydor, G. Cofta, B. Doczekalska, A. Bonenberg, Fungi in mycelium-based composites: usage and recommendations, *Materials (Basel)* (2022) 15, <https://doi.org/10.3390/ma15186283>.
- [12] S. Vandeloock, E. Elsacker, A. van Wylick, L. de Laet, E. Peeters, Current state and future prospects of pure mycelium materials, *Fungal Biol. Biotechnol.* 8 (2021), <https://doi.org/10.1186/s40694-021-00128-1>.
- [13] K. Rafiee, G. Kaur, S.K. Brar, Fungal biocomposites: how process engineering affects composition and properties? *Bioresour. Technol. Rep.* 14 (2021) <https://doi.org/10.1016/j.biteb.2021.100692>.
- [14] E. Elsacker, S. Vandeloock, J. Brancart, E. Peeters, L. de Laet, Mechanical, physical and chemical characterisation of mycelium-based composites with different types of lignocellulosic substrates, *PLoS ONE* 14 (2019) 1–20, <https://doi.org/10.1371/journal.pone.0213954>.
- [15] N. Attias, A. Livne, T. Abitbol, State of the art, recent advances, and challenges in the field of fungal mycelium materials: a snapshot of the 2021 Mini Meeting, *Fungal Biol. Biotechnol.* 8 (2021), <https://doi.org/10.1186/s40694-021-00118-3>.
- [16] D.A. Jaramillo, M.J. Méndez, G. Vargas, E.E. Stashenko, A.M. Vasco-Palacios, A. Ceballos, N.H. Caicedo, Biocatalytic potential of native basidiomycetes from Colombia for flavour/aroma production, *Molecules* (2020) 25, <https://doi.org/10.3390/molecules25184344>.
- [17] R. Lelivelt, G. Lindner, P. Teuffel, H. Lamers, The production process and compressive strength of Mycelium-based materials, in: First International Conference on Bio-Based Building Materials, 2015: pp. 1–6. www.tue.nl/taverne.
- [18] W. Rasband, ImageJ, (n.d.). <https://imagej.nih.gov/ij/>.
- [19] Origin(Pro), Version 2017, (n.d.). <https://www.originlab.com/>.
- [20] A.R. Sahito, R.B. Mahar, Z. Siddiqui, K.M. Brohi, Estimating calorific values of lignocellulosic biomass from volatile and fixed solids, *Int. J. Biomass And Renew.* 2 (2013) 1–6.
- [21] ASTM International, Standard test method for dimensions and density of preformed block and board-type thermal insulation; ASTM C 303 –02, n.d. <https://doi.org/10.1520/C0303-02>.
- [22] F.V.W. Appels, S. Camere, M. Montalti, E. Karana, K.M.B. Jansen, J. Dijksterhuis, P. Krijgheld, H.A.B. Wösten, Fabrication factors influencing mechanical, moisture- and water-related properties of mycelium-based composites, *Mater. Des.* 161 (2019) 64–71, <https://doi.org/10.1016/j.matdes.2018.11.027>.
- [23] W.D. Powrie, H. Chiu Wu, V.P. Molund, Browning reaction systems as sources of mutagens and antimutagens, *Environ. Health Perspect.* 67 (1986) 47–54, <https://doi.org/10.1289/ehp.866747>.
- [24] I.S. Santos, B.L. Nascimento, R.H. Marino, E.M. Sussuchi, M.P. Matos, S. Griza, Influence of drying heat treatments on the mechanical behavior and physico-chemical properties of mycelial biocomposite, *Compos. B Eng.* (2021) 217, <https://doi.org/10.1016/j.compositesb.2021.108870>.
- [25] N.L. Glass, C. Rasmussen, M.G. Roca, N.D. Read, Hyphal homing, fusion and mycelial interconnectedness, 12 (2004). <https://doi.org/10.1016/j.tim.2004.01.007>.
- [26] K. Joshi, M.K. Meher, K.M. Poluri, Fabrication and characterization of bioblocks from agricultural waste using fungal mycelium for renewable and sustainable applications, *ACS Appl. Bio. Mater.* 3 (2020) 1884–1892, <https://doi.org/10.1021/acsabm.9b01047>.
- [27] G. Silva Ribeiro, M.K. Conceição Monteiro, J. Rodrigues do Carmo, R. da Silva Pena, R. Campos Chisté, Peach palm flour: production, hygroscopic behaviour and application in cookies, *Heliyon* 7 (2021), <https://doi.org/10.1016/j.heliyon.2021.e07062>.
- [28] G. Marrugo, C.F. Valdés, F. Chejne, Characterization of Colombian agroindustrial biomass residues as energy resources, *Energy and Fuels* 30 (2016) 8386–8398, <https://doi.org/10.1021/acs.energyfuels.6b01596>.
- [29] A. Kumar, Y. Singh Negi, V. Choudhary, N.Kant Bhardwaj, Characterization of cellulose nanocrystals produced by acid-hydrolysis from sugarcane bagasse as agro-waste, *J. Mater. Phys. Chem.* 2 (2020) 1–8, <https://doi.org/10.12691/jmpc-2-1-1>.
- [30] M.B. Pires, E.R. Amante, A.S. Lopes, A.M. da C-Rodrigues, L.H.M. da SILVA, Peach palm flour (*Bactris gasipae* KUNTH): potential application in the food industry,

- Food Sci. Technol. (Brazil) 39 (2019) 613–619, <https://doi.org/10.1590/fst.34617>.
- [31] J. Zhuang, M. Li, Y. Pu, A.J. Ragauskas, C.G. Yoo, Observation of potential contaminants in processed biomass using fourier transform infrared spectroscopy, *Appl. Sci.* 10 (2020) 1–13, <https://doi.org/10.3390/app10124345>.
- [32] W. Sun, M. Tajvidi, C. Howell, C.G. Hunt, Functionality of surface mycelium interfaces in wood bonding, *ACS Appl. Mater. Interfaces* 12 (2020) 57431–57440, <https://doi.org/10.1021/acsami.0c18165>.
- [33] T. Hong, J.Y. Yin, S.P. Nie, M.Y. Xie, Applications of infrared spectroscopy in polysaccharide structural analysis: progress, challenge and perspective, *Food Chem. X* 12 (2021), 100168, <https://doi.org/10.1016/j.fochx.2021.100168>.
- [34] M. Chylinska, B. Kruk, A. Zdunek, Combining FT-IR spectroscopy and multivariate analysis for qualitative and quantitative analysis of the cell wall composition changes during apples development, *Carbohydr. Polym.* 115 (2015) 93–103, <https://doi.org/10.1016/j.carbpol.2014.08.039>.
- [35] E. Gallio, P. Zanatta, D.D. Ribes, M. Lazarotto, D.A. Gatto, R. Beltrame, Fourier transform infrared spectroscopy in treated woods deteriorated by a white rot fungus, *Maderas: Ciencia y Tecnologia* 20 (2018) 479–488, <https://doi.org/10.4067/S0718-221X2018005031701>.
- [36] D. Ciolacu, F. Ciolacu, V.I. Popa, Amorphous cellulose-structure and characterization, *Cellulose Chem. Technol.* 45 (2011) 13–21.
- [37] I. Kubovský, D. Kačková, F. Kačík, Structural changes of Oak wood main components caused by thermal modification, *Polymers (Basel)* (2020), <https://doi.org/10.3390/polym12020485>.
- [38] C. Popescu, G. Singurel, M. Popescu, C. Vasile, S. Dimitris, S. Willför, Vibrational spectroscopy and X-ray diffraction methods to establish the differences between hardwood and softwood, *Carbohydr. Polym.* 77 (2009) 851–857, <https://doi.org/10.1016/j.carbpol.2009.03.011>.
- [39] K.K. Pandey, A.J. Pitman, FTIR studies of the changes in wood chemistry following decay by brown-rot and white-rot fungi, *Int. Biodeterior. Biodegradation* 52 (2003) 151–160, [https://doi.org/10.1016/S0964-8305\(03\)00052-0](https://doi.org/10.1016/S0964-8305(03)00052-0).
- [40] ASTM International, Standard test method for determining anaerobic biodegradation of plastic materials under accelerated landfill conditions; ASTM D5526-18. (n.d.). <https://doi.org/10.1520/D5526-18>.
- [41] E.U. Remigi, C.A. Buckley, Co-digestion of high strength/toxic organic effluents in anaerobic digesters at wastewater treatment works, 2006.
- [42] N. Nwokolo, P. Mukumba, K. Obileke, M. Enebe, Waste to energy: a focus on the impact of substrate type in biogas production, *Processes* 8 (2020) 1–21, <https://doi.org/10.3390/pr8101224>.
- [43] C.P. Pabón-Pereira, H.V.M. Hamelers, I. Matilla, J.B. van Lier, New insights on the estimation of the anaerobic biodegradability of plant material: identifying valuable plants for sustainable energy production, *Processes* 8 (2020), <https://doi.org/10.3390/pr8070806>.
- [44] L. Janke, A. Leite, M. Nikolausz, T. Schmidt, J. Liebetrau, M. Nelles, W. Stinner, Biogas production from sugarcane waste: assessment on kinetic challenges for process designing, *Int. J. Mol. Sci.* 16 (2015) 20685–20703, <https://doi.org/10.3390/ijms160920685>.
- [45] P. Kumar, D.M. Barrett, M.J. Delwiche, P. Stroeve, Methods for pretreatment of lignocellulosic biomass for efficient hydrolysis and biofuel production, *Ind. Eng. Chem. Res.* 48 (2009) 3713–3729, <https://doi.org/10.1021/ie801542g>.
- [46] M. Jones, T. Huynh, C. Dekiwadia, F. Daver, S. John, Mycelium composites: a review of engineering characteristics and growth kinetics, *J. Bionanosci.* 11 (2017) 241–257, <https://doi.org/10.1166/jbns.2017.1440>.
- [47] M.D. Fricker, L.L.M. Heaton, N.S. Jones, L. Boddy, The mycelium as a network, *Microbiol. Spectr.* 5 (2017), <https://doi.org/10.1128/microbiolspec.funk-0033-2017>.